Global Journal of Engineering and Technology Advances
eISSN: 2582-5003
Cross Ref DOI: 10.30574/gjeta
Journal homepage: https://gjeta.com/

(Research Article)

Check for updates

FAILURE ANALYSIS AND MATERIAL DEGRADATION OF REUSABLE LAUNCH VEHICLE STRUCTURES

Durojaye Rasheed Olalekan [1,*], Suleiman Meimuna [2], Odunaiya Ganiyu Ayodele [2], Kehinde Michael Adebayo [2], John Daniel Ekanem [2] and Agbedun Sola Stephen [2]

[1] Projects, Planning and Strategic Development Division, Bola Ahmed Tinubu Centre for Space Transport and Propulsion, Epe Lagos Nigeria.
[2] Rocket Systems Engineering Division, Bola Ahmed Tinubu Centre for Space Transport and Propulsion, Epe Lagos Nigeria.
* Corresponding Author

ORCID Details
Durojaye Rasheed Olalekan: https://orcid.org/0009-0005-2009-3632

Global Journal of Engineering and Technology Advances, 2026, 28(03), 114–124

Publication history: Received on 31 July 2026; revised on 05 September 2026; accepted on 08 September 2026

Article DOI: https://doi.org/10.30574/gjeta.2026.28.3.0240

ABSTRACT

This project investigates the failure analysis and material degradation mechanisms in reusable launch vehicle (RLV) structures, addressing the challenges posed by extreme thermo-mechanical and environmental loads during multiple mission cycles. Unlike expendable systems, RLVs such as those developed by SpaceX and NASA must endure hypersonic heating, thermal gradients up to 1500°C, cyclic pressurization, vibrations, impacts, and oxidative environments, leading to degradation modes including fatigue cracking, creep, oxidation-induced embrittlement, delamination, and buckling. The study reviews key structural challenges, failure mechanisms, and mitigation strategies, emphasizing the need for advanced materials, predictive modelling, and non-destructive evaluation to ensure safety, reliability, and cost-effectiveness. Through a comprehensive analysis, this work provides insights into enhancing structural durability for sustainable space transportation.

Two aluminum-based composite material series, designated as Sample A and Sample B, were obtained as representative candidate materials for RLV structural components. Sample A were material used to construct the launch vehicle while sample B were materials extracted from the launch vehicle after flight and recovery. Each series was prepared as five individual specimens, labelled 1 to 5 (i.e. A1-A5 and B1-B5), giving ten specimens in total.

Four mechanical tests were carried out to comprehensively characterize the specimens against the degradation mechanisms before and after flight.

Flexural (three-point bend) testing to evaluate bending strength and stiffness, relevant to structural panels and fuselage sections under aerodynamic and mechanical bending loads. Hardness testing to evaluate surface resistance to indentation, relevant to resistance against surface damage and as an indirect indicator of wear performance. Impact testing to evaluate the energy absorbed prior to fracture under sudden loading, relevant to shock events such as launch vibration and landing impact. Wear testing to evaluate resistance to surface material loss under sliding contact, relevant to repeated friction and surface exposure across reuse cycles. Together, these four tests were considered to represent all mechanical tests applicable within the scope and equipment available for this study, providing a comprehensive mechanical performance profile for each specimen.

Keywords: Creep, Delamination, Hypersonic, Oxidation, Thermal Protection System, Thermal Fatigue, Reusable Launch Vehicle.

1 INTRODUCTION

The global aerospace industry is undergoing a revolutionary transition from expendable launch systems toward reusable space transportation systems. Historically, **expendable launch vehicles (ELVs)** were discarded after a single mission, resulting in high operational costs and significant material waste. The economic inefficiency of such systems has driven innovation toward reusable launch vehicles (RLVs), which are designed to survive multiple launch, ascent, re-entry, and landing cycles [1].

Reusable launch vehicles significantly reduce cost per launch and increase mission frequency. Companies such as SpaceX, Blue Origin, and governmental agencies like NASA have demonstrated the economic and operational feasibility of partial and fully reusable systems [2], [3],[4]. However, achieving reliable reuse introduces complex engineering challenges, especially in structural durability and material performance [5],[6]. Unlike conventional aircraft structures, RLV structures are subjected to: Hypersonic aerodynamic heating, Extreme thermal gradients (up to 1500°C in some regions), Cyclic pressurization loads, Vibrational and acoustic loads during launch, Mechanical impact during landing Oxidative and corrosive atmospheric environments [7], [8], [9]. These conditions create a multi-physics loading environment involving thermomechanical coupling, dynamic stress waves, and microstructural evolution [10], [11].

Reusable Launch Vehicle (RLV) structures operate under significantly more severe service conditions compared to conventional aircraft systems. Unlike traditional aircraft, which primarily experience subsonic or supersonic aerodynamic environments, RLVs are exposed to extreme thermo-mechanical and environmental loads during launch, orbital operation, re-entry, and landing phases. These demanding conditions accelerate material degradation and increase the risk of structural failure if not properly addressed during design and material selection. One of the primary challenges encountered by RLV structures is **hypersonic aerodynamic heating.** During atmospheric re-entry, vehicles travel at hypersonic velocities (Mach 5 and above), resulting in intense aerodynamic compression and friction between the vehicle surface and atmospheric gases. This interaction generates extremely high surface temperatures, which can induce severe thermal stresses, oxidation, and microstructural degradation in structural materials. The thermal protection system (TPS) and load-bearing components must therefore withstand sustained exposure to elevated temperatures without significant loss of mechanical integrity. In addition to aerodynamic heating, RLV structures are subjected to **extreme thermal gradients,** with temperatures reaching up to approximately 1500°C in certain regions. These gradients occur due to uneven heating across the vehicle surface and rapid transitions between high-temperature and relatively cooler internal structural regions. Such non-uniform temperature distribution produces differential thermal expansion, leading to internal stress development. Repeated exposure to these gradients may result in thermal fatigue, crack initiation, delamination in composite materials, and creep deformation in high-temperature alloys.

RLVs also experience **cyclic pressurization loads,** particularly in fuel tanks and pressurized compartments. During each mission, internal pressure fluctuates significantly due to fueling, ascent, orbital operations, and descent. These cyclic stresses contribute to fatigue damage accumulation, especially at stress concentration sites such as joints, welds, and fastener locations. Over multiple missions, fatigue crack propagation may compromise structural reliability if not detected and mitigated. Furthermore, during launch, RLV structures are exposed to **intense vibrational and acoustic loads** generated by rocket propulsion systems. High-frequency vibrations and acoustic shock waves induce dynamic stresses throughout the vehicle structure. These loads can cause micro-crack formation, fastener loosening, material delamination, and progressive structural weakening. The combined effect of vibration and high temperature further accelerates degradation mechanisms. Another critical loading condition arises from **mechanical impact during landing.** Reusable vehicles are designed to withstand multiple landing cycles, which introduce impact forces and localized stress concentrations at landing gear attachments and structural interfaces. Repeated impact loading may result in plastic deformation, crack initiation, or structural fatigue failure over time. Additionally, RLV materials are subjected to **oxidative and corrosive atmospheric environments,** particularly during high-temperature re-entry. Elevated temperatures accelerate oxidation reactions in metallic components, leading to scale formation, surface embrittlement, and thickness reduction. Environmental exposure may also promote stress corrosion cracking and environmentally assisted fracture mechanisms, especially in high-strength alloys. Collectively, these operational conditions create a highly complex **multi-physics loading environment**. The structural materials must simultaneously endure thermomechanical coupling, where thermal and mechanical stresses interact; dynamic stress wave propagation during launch and landing; and continuous microstructural evolution due to prolonged exposure to high temperatures and cyclic loading. Microstructural changes such as grain growth, phase transformation, dislocation accumulation, and oxidation-induced embrittlement significantly influence long-term material performance. Therefore, failure analysis of RLV materials requires a comprehensive understanding of coupled thermal, mechanical, and environmental degradation mechanisms. The interaction of these factors plays a critical role in crack initiation, propagation, and eventual structural failure, making advanced material characterization and life prediction methodologies essential for ensuring structural integrity and mission safety.

The repeated exposure of reusable launch vehicle (RLV) structures to extreme thermo-mechanical and environmental conditions results in progressive and cumulative material degradation. Unlike single-use aerospace systems, RLV components must endure multiple launch and re-entry cycles, which significantly increases the likelihood of damage accumulation over time. As a consequence, structural integrity may deteriorate through several interacting degradation mechanisms, including: Fatigue crack initiation and propagation, Thermal fatigue cracking, Creep deformation, Oxidation-induced embrittlement, Composite delamination, Buckling instability [12],[13],[14],[15],[16]. Among these mechanisms, **fatigue crack initiation and propagatio**n represents one of the most critical failure modes in reusable aerospace structures. Cyclic mechanical loading during pressurization, launch vibrations, and landing impact produces repeated stress fluctuations within the material. Over time, localized stress concentrations particularly at welds, joints, fastener holes, and geometric discontinuities promote micro crack initiation. Once initiated, these cracks progressively propagate under continued cyclic loading until catastrophic fracture occurs. Fatigue damage is particularly dangerous because it may develop without significant macroscopic deformation, making early detection challenging.

In addition to mechanical fatigue, RLV structures are highly susceptible to **thermal fatigue cracking** due to repeated heating and cooling cycles during ascent and re-entry. Rapid temperature fluctuations generate alternating thermal expansion and contraction within the material. If thermal strains are constrained, internal stresses develop, leading to crack nucleation at the surface or within grain boundaries. Over multiple mission cycles, these cracks may grow and coalesce, significantly reducing load-bearing capacity.

Another time-dependent degradation mechanism is **creep deformation**, which becomes significant at elevated temperatures. When structural materials are subjected to sustained stresses at high temperatures such as during atmospheric re-entry, they may undergo slow, progressive plastic deformation even if the applied stress is below the material's yield strength. Creep can lead to dimensional instability, stress redistribution, grain boundary void formation, and eventual creep rupture. For high-temperature alloys and thermal protection materials, creep resistance is therefore a critical design consideration.

High-temperature exposure also promotes **oxidation-induced embrittlement**. At elevated temperatures, metallic materials react with atmospheric oxygen, forming oxide scales on their surfaces. While some oxide layers may provide protective effects, prolonged exposure can lead to scale spallation, thickness reduction, and internal oxidation. More critically, oxygen diffusion into the material can alter microstructural characteristics, reduce ductility, and increase brittleness. This embrittlement raises susceptibility to crack initiation and rapid fracture under mechanical loading.

For composite materials commonly used in aerospace structures, **delamination** is a significant degradation mechanism. Composite laminates consist of multiple bonded layers, and exposure to thermal gradients, cyclic stresses, and impact loading can weaken interlaminar bonding. Delamination reduces stiffness and load transfer efficiency between layers, potentially leading to sudden structural failure without extensive visible damage.

Finally, **buckling instability** may occur due to combined thermal and mechanical stresses. Thin-walled aerospace structures are particularly vulnerable to compressive stresses generated by thermal gradients and aerodynamic loads. If the compressive stress exceeds the critical buckling threshold, sudden structural instability may occur, resulting in significant deformation or collapse. Buckling is especially critical in panels, fuselage sections, and thermal protection components subjected to high temperature differentials.

Overall, these degradation mechanisms rarely occur independently. Instead, they interact within a complex multi-physics environment, where thermal, mechanical, and environmental factors collectively accelerate damage accumulation. The coupling of fatigue, creep, oxidation, and microstructural evolution significantly influences the long-term reliability and service life of RLV structures. Therefore, comprehensive failure analysis must consider not only individual mechanisms but also their synergistic interactions to accurately predict structural lifespan and prevent catastrophic failure.

Understanding the mechanisms behind these failure processes is essential to ensuring safety, reliability, and cost-effectiveness [17]. Failure analysis provides systematic procedures for identifying the root causes of structural damage. Material degradation studies enable prediction of long-term behavior under cyclic service conditions. Together, these disciplines form the foundation of structural life prediction in reusable aerospace systems [18],[19].

2 MATERIAL AND METHOD

2.1 Materials

2.1.1 Specimens

Two aluminum-based composite material series, designated as Sample A and Sample B, were obtained as representative candidate materials for RLV structural components. Sample A were material used to construct the launch vehicle while sample B were materials extracted from the launch vehicle after flight and recovery. Each series was prepared as five individual specimens, labelled 1 to 5 (i.e. A1-A5 and B1-B5), giving ten specimens in total.

2.1.2 Equipment

Four mechanical tests were selected to comprehensively characterize the specimens against the degradation mechanisms:

- Flexural (three-point bend) testing to evaluate bending strength and stiffness, relevant to structural panels and fuselage sections under aerodynamic and mechanical bending loads. Static was performed on an Instron 3369 Universal Testing Machine.
- Hardness testing to evaluate surface resistance to indentation, relevant to resistance against surface damage and as an indirect indicator of wear performance. Surface hardness was assessed with a SOONDA SKD 552 Leeb rebound hardness tester.
- Impact testing to evaluate the energy absorbed prior to fracture under sudden loading, relevant to shock events such as launch vibration and landing impact. Impact resistance was assessed with a Hounsfield Balanced Impact Machine of the pendulum type.
- Wear testing to evaluate resistance to surface material loss under sliding contact, relevant to repeated friction and surface exposure across reuse cycles. Sliding wear behavior was assessed on a wear testing apparatus operating on the pin on disc principle, with volumetric loss interpreted through the Archard wear relation.

Together, these four tests were considered to represent all mechanical tests applicable within the scope and equipment available for this study, providing a comprehensive mechanical performance profile for each specimen.

2.2 Method

2.2.1 Fabrication

Specimens were extracted at the workshop using arc-saw machine and surface polishing was caried out on them. Each test was carried out following standard mechanical testing procedures consistent with recognized ASTM/ISO testing conventions for flexural, hardness, impact, and wear testing of metallic and composite materials. For each specimen, replicate readings were taken (two runs for flexural testing; five readings each for hardness and impact testing) and averaged to obtain a representative value, reducing the influence of localized material variation on the reported result. Wear testing was carried out once per specimen.

2.2.2 Three Point Flexural Test

Flexural testing was carried out on the Instron 3369 configured in a three-point bending arrangement. Test on 5 samples of specimen A and 5 samples of specimen B were carried out. The load deflection output was used to calculate the maximum flexural stress, the flexural elastic modulus, the flexural stress at break, the energy absorbed to fracture, and the strain at maximum stress for both samples.

2.2.3 Hardness Test

Leeb rebound hardness measurements were taken at different locations across the face of the samples using the SOONDA SKD 552 tester. The Leeb method is standardized under ISO 16859-1 for metallic materials. Hardness testing was conducted on two different aluminum samples, designated Sample A and Sample B, with five specimens tested from each sample. The objective was to compare the hardness characteristics of the two aluminum materials and determine the variation in hardness within each sample. A total of 10 specimens were prepared and subjected to hardness testing using a suitable hardness testing machine. The specimens were properly cleaned and positioned on the testing surface before applying the specified test load. For each sample, five individual hardness measurements were taken under the same testing conditions to ensure a meaningful comparison.

2.2.4 Pendulum Impact Test

Impact testing was carried out to evaluate the ability of two different aluminum samples, designated **Sample A** and **Sample B**, to absorb energy under sudden loading. The test was performed using an appropriate impact testing machine, such as a Charpy impact tester, with **five specimens tested from each sample**.

The specimens were prepared to the required dimensions and notched where applicable. Each specimen was securely positioned on the impact-testing machine, and the pendulum was released from a predetermined height. The pendulum fractured the specimen, and the **impact energy absorbed during fracture** was obtained from the machine.

2.2.5 Sliding Wear Test

Sliding wear testing was carried out to evaluate the resistance of aluminium specimens to material loss resulting from sliding contact and friction. The test involved two different aluminium samples, **Sample A and Sample B**, with **five specimens tested from each sample**. Prior to testing, the specimens were prepared and their surfaces cleaned to remove dirt, grease, and other contaminants. Each specimen was weighed and mounted on the wear-testing machine. A specified normal load was applied while the specimen was subjected to sliding motion against the counter surface for a predetermined sliding distance and speed. After testing, the specimens were cleaned and weighed again. The difference between the initial and final masses was used to determine the material lost during the wear process. The **wear rate** of each specimen was calculated from the measured mass loss and the specified test conditions. The results from the five specimens of each sample were then used to determine the average wear performance.

3 RESULTS AND DISCUSSION

This chapter presents the results of the mechanical testing carried out on the material samples selected to represent candidate structural materials for reusable launch vehicle (RLV) construction. Two aluminum-based composite material series, designated Sample A and Sample B, were obtained and subjected to the full range of mechanical tests applicable to the study: flexural (three-point bend) testing, hardness testing, impact testing, and wear testing. Each series comprised five specimens (1-5), (A1-A5 and B1-B5) had been fully tested and are reported here. The results are presented test-by-test, followed by a comparative discussion of Sample A against Sample B.

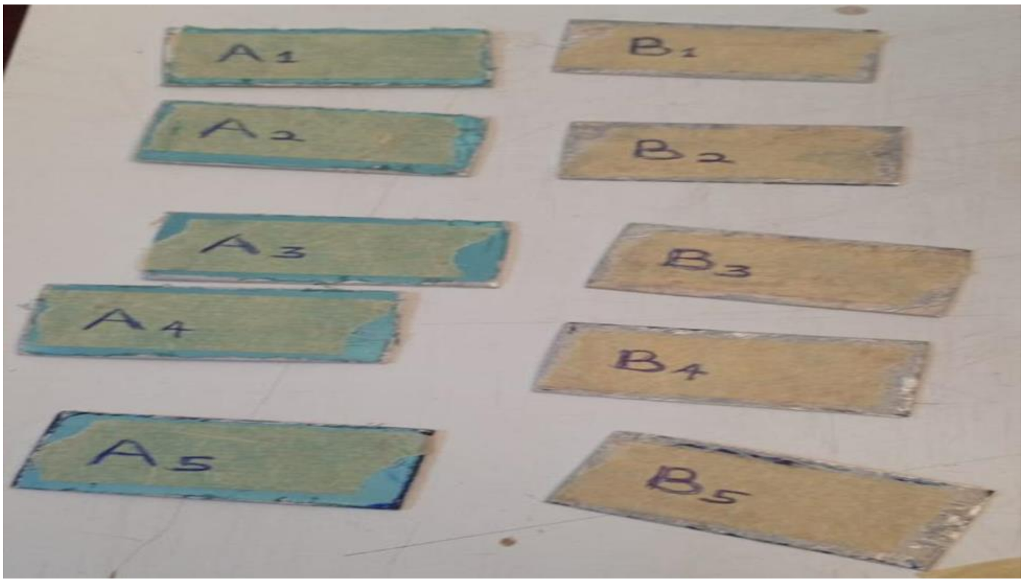

Figure 1: Specimens of two different Aluminum Samples A and B

3.1 Flexural Test Results

The flexural (three-point bend) test was conducted to evaluate the resistance of each specimen to bending loads, a loading condition relevant to RLV panels and fuselage sections during ascent, aerodynamic loading, and structural bending. Table 1 presents the maximum flexural stress recorded for each specimen.

Table 1: Flexural Test Result for Virgin (A) vs Flown (B) materials

Specimen Pair	Virgin (A) Max Stress (MPa)	Flown (B) Max Stress (MPa)
1	84.89	88.56
2	82.84	86.95
3	81.48	85.72
4	80.75	83.64
5	78.63	81.53
Mean	81.72	85.28

The Flown sample therefore exhibited a higher average maximum flexural stress**,** with an increase of approximately **3.56 MPa**, or **4.36%**, relative to the Virgin sample. This indicates that, under the conditions of the flexural test, the Flown aluminium specimens demonstrated slightly greater resistance to bending-induced failure than the Virgin specimens. The improvement was observed consistently across all five specimen pairs, with the Flown sample producing a higher maximum stress in every case. The increase in flexural strength may be associated with differences in the material's microstructure, thermal history, residual stresses, or changes induced during the service/flight condition, depending on the specific history of the Flown specimens. However, the flexural results alone cannot establish the exact cause of the increase.

Figure 2: Universal Testing Machine used for Flexural Testing

3.2 Hardness Test Results

Table 2: Hardness - Virgin (A) vs Flown (B) Comparison

Specimen Pair	Virgin (A) HV	Flown (B) HV
1	41.12	42.38
2	38.19	43.70
3	41.33	43.46
4	40.23	42.55
5	39.75	43.21
Mean	40.12	43.06

Hardness testing was carried out to assess the resistance of each specimen's surface to indentation, which relates to the material's ability to resist surface damage and wear during repeated handling, friction, and contact loading. Table 2 presents the average hardness value recorded for each specimen.

The results show that the **Virgin (A)** specimens recorded hardness values between **38.19 and 41.33 HV**, with a mean hardness of **40.12 HV**. In comparison, the **Flown (B)** specimens recorded higher hardness values ranging from **42.38 to 43.70 HV**, with a mean value of **43.06 HV**. The mean hardness of the Flown sample is therefore **2.94 HV higher** than that of the Virgin sample, representing an increase of approximately **7.33%.** This increase was observed consistently across all five specimen pairs, as each Flown specimen recorded a higher hardness value than its corresponding Virgin specimen. The higher hardness of the Flown sample indicates that the material developed **greater resistance to localized plastic deformation** following its service or flight history. In aluminium alloys, such a change can be associated with factors such as strain hardening, thermal exposure, microstructural changes, precipitation effects, or other changes occurring during the material's service history [20], [21].

Figure 3: Leeb Portable Hardness Tester

3.3 Impact Test Results

Impact testing was carried out to determine the energy absorbed by each specimen prior to fracture under sudden loading, which is directly relevant to RLV structures that must survive shock loading events such as launch vibration and landing impact. the comparison of the **impact energy values** obtained from five specimen pairs of the **Virgin (A)** and **Flown (B)** aluminum samples. The impact test was used to evaluate the ability of the materials to absorb energy under sudden loading before fracture. Table 3 presents the average impact energy recorded for each specimen.

Table 3: Impact Energy - Virgin (A) vs Flown (B) Comparison

Specimen Pair	Virgin (A) (J/mm^2)	Flown (B) (J/mm^2)
1	0.1813	0.2796
2	0.0416	0.1291
3	0.0403	0.1244
4	0.0512	0.1278
5	0.0341	0.1322
Mean	0.0697	0.1586

Figure 4: Hounsfield Balanced Impact Testing Machine

3.4 Wear Test Results

Table 4 compares the **wear resistance of virgin aluminum (A)** with that of the **flown aluminum (B)**. The results indicate that the flown specimens have a higher measured wear-resistance value than the virgin specimens.

Table 4: Wear Resistance - Virgin (A) vs Flown (B)

Specimen Pair	Virgin (A) (N.m/mm^3)	Flown (B) (N.m/mm^3)
1	41.68	48.35
2	40.52	47.44
3	42.05	48.63
4	41.61	47.82
5	40.55	47.48
MEAN	41.28	47.95

The virgin specimens recorded wear-resistance values between 40.52 and 42.05 N·m/mm^3**,** while the flown specimens recorded values between 47.44 and 48.63 N·m/mm^3**.** The mean wear-resistance values were 41.28 N·m/mm^3 for the virgin material and 47.95 N·m/mm^3 the flown material for. Therefore, the flown aluminium exhibited approximately a **16.13% higher wear-resistance value** than the virgin aluminium.

The reported N·m/mm^3 parameter is the wear-resistance index, for which a higher value represents better resistance to material removal, the result indicates that the flown aluminum has approximately 16.13% greater wear resistance than the virgin aluminum.

This improvement could be associated with changes in the material resulting from its service history. Possible contributing factors include:

- **Strain hardening:** Repeated mechanical and vibrational loading during flight may have increased resistance to plastic deformation at the surface.
- **Microstructural modification:** Operational thermal and mechanical exposure may have altered the microstructure and consequently the wear behavior.
- **Changes in hardness:** If the hardness test results also show an increase in hardness for the flown material, this may contribute to its improved resistance to abrasive or adhesive wear.
- **Surface modification:** Flight exposure can alter surface roughness, oxide-film characteristics and other surface properties, which can influence wear behavior.

- **Residual stresses:** Service loading and thermal cycling may introduce residual stresses that affect the response of the surface during sliding.

The increased wear resistance is particularly interesting when considered alongside the higher hardness of the flown material.

3.5 Comparative Discussion: Sample A versus Sample B

Table 5: Summary - Virgin vs Flown, Mean Change Across All Tests

Test	Virgin (A) Mean	Flown (B) Mean
Flexural Strength (MPa)	81.72	85.28
Hardness (HV)	40.12	43.06
Impact Energy (J/mm^2)	0.0697	0.1586
Wear Resistance (N.m/mm^3)	41.28	47.95

Table 5 provides a comparative summary of the mean mechanical and tribological properties of Sample A (Virgin) and Sample B (Flown). The table makes it possible to evaluate the overall effect of the flight/service environment on the aluminum material.

3.6 Comparative Discussion of Sample A and Sample B

The results show that Sample B (Flown) recorded higher mean values than Sample A (Virgin) in all four tests: flexural strength, hardness, impact energy, and wear resistance. This indicates that the flown material experienced measurable changes in its mechanical and wear characteristics during service.

3.6.1 Flexural Strength

The mean flexural strength increased from 81.72 MPa for the virgin sample to 85.28 MPa for the flown sample, representing a 4.36% increase. This relatively moderate increase suggests that service exposure produced some improvement in the material's resistance to bending or flexural deformation. Possible factors include strain hardening, changes in microstructure, residual stresses, or thermal exposure during service. However, the increase is relatively small compared with the changes observed in impact energy and wear resistance. Therefore, the flight environment appears to have had a limited but measurable influence on flexural strength.

3.6.2 Hardness

The mean hardness increased from 40.12 HV to 43.06 HV, corresponding to a 7.33% increase. The increase in hardness indicates that the flown material became more resistant to localized plastic deformation. This could result from strain hardening caused by repeated operational loading, microstructural changes, or thermal effects experienced during service. The increase in hardness may also have contributed to the improved wear resistance observed for Sample B. Nevertheless, wear behavior is influenced by several factors, so the relationship should not be regarded as being caused by hardness alone.

3.6.3 Impact Energy

The most significant change occurred in the impact test. The mean impact energy increased from 0.0697 J/mm^2 for the virgin material to 0.1586 J/mm^2 for the flown material. This represents an increase of approximately 127.55%, meaning that the flown specimens absorbed considerably more energy under the specified impact-test conditions. This result suggests that the flown material exhibited an enhanced ability to absorb sudden loading before failure. Such behavior may be associated with microstructural modification, changes in grain structure, precipitate evolution, residual stress redistribution, or other service-induced changes. The magnitude of this change is considerably greater than those observed for flexural strength and hardness and therefore represents one of the most notable differences between the two material conditions.

3.6.4 Wear Resistance

The mean wear-resistance value increased from **41.28 N·m/mm^3 for Sample A to 47.95 N·m/mm^3 for Sample B**, representing an improvement of approximately **16.13%**.

Since the reported parameter is defined as a **wear-resistance index**, with higher values representing greater resistance to material loss, the result indicates that the flown material had superior wear resistance under the test conditions. The improvement may be associated with the increased hardness of the flown material, as well as changes in surface condition, microstructure, oxide formation, residual stress and other service-induced effects.

3.6.5 Overall Comparative Assessment

The results demonstrate that the flown aluminum exhibited improved measured properties relative to the virgin material:

- **Flexural strength:** increased by **4.36%**
- **Hardness:** increased by **7.33%**
- **Impact energy:** increased by **127.55%**
- **Wear resistance:** increased by **16.13%**

The impact energy showed the largest relative change, followed by wear resistance, hardness and flexural strength. This indicates that the service history had a particularly pronounced influence on the impact response of the material.

4 CONCLUSION

The comparative investigation of the virgin and flown aluminium specimens has demonstrated that exposure to the operational environment resulted in measurable changes in the mechanical and tribological properties of the material. The results obtained from the flexural strength, hardness, impact energy and wear-resistance tests consistently showed higher mean values for the flown specimens compared with the virgin specimens.

The mean flexural strength increased from 81.72 MPa for the virgin material to 85.28 MPa for the flown material, representing an improvement of approximately 4.36%. Similarly, the mean hardness increased from 40.12 HV to 43.06 HV, corresponding to a 7.33% increase. The most pronounced change was observed in the impact energy, which increased from 0.0697 J/mm^2 for the virgin specimens to 0.1586 J/mm^2 for the flown specimens, representing an increase of approximately 127.55%. The reported wear-resistance parameter also increased from 41.28 to 47.95 $N{\cdot}m/mm^3$, corresponding to an improvement of approximately 16.13%, assuming that higher values represent greater wear resistance.

The overall improvement observed in the flown material suggests that its service history may have induced changes in its microstructure, surface condition, residual stress state and mechanical response. Repeated mechanical loading, vibration, thermal cycling and other operational conditions may have contributed to these changes through mechanisms such as strain hardening and microstructural evolution. The increase in hardness may also have contributed to the observed improvement in wear resistance, although wear behaviour is influenced by several factors beyond hardness alone.

In conclusion, the study establishes that flight/service exposure produced significant and measurable modifications in the investigated aluminium material, with improvements recorded in flexural strength, hardness, impact energy and the reported wear-resistance parameter. The findings demonstrate the importance of evaluating the actual service history and material condition of aerospace components rather than relying exclusively on properties obtained from unused or virgin materials when assessing structural performance and serviceability.

STATEMENTS ON COMPLIANCE WITH ETHICAL STANDARDS

Acknowledgments

We sincerely appreciate the Centre for Energy research and Development (CERD) Obafemi Awolowo University Ile-Ife for the use of their facilities during this research work. Also, we appreciate Bola Ahmed Tinubu Cntre for Space Transport and Propulsion for the use of their laboratory equipment and facilities during this research work.

Funding Source

The research was funded through the authors' joint research and development fund pool

Disclosure of conflict of interest

There are no conflicts of interest.

REFERENCES

[1] Fernández, L. A., & Wiedemann, C. (2022). Analysis of space launch vehicle failures and post-mission disposal statistics. Aerotecnica Missili Spazio, 101(1), 1–12

[2] Brociek, R., et al. (2023). Reconstruction of aerothermal heating for the thermal protection system of a reusable launch vehicle. Applied Thermal Engineering, 219, Article 119405.

[3] Thomas, D. (2024). SpaceX Starship's reusability revolution: Mitigating engine failure risks through advanced failure analysis. Journal of Failure Analysis and Prevention, 24(3), 456–472.

[4] Rauh, C., et al. (2025). DLR concepts of advanced thermal protection systems for reusable cryogenic propellant tanks [Conference presentation]. 3rd International Conference on Flight Vehicles, Aerothermodynamics and Re-entry (FAR).

[5] Yang, Z., et al. (2023). Life assessment of thermomechanical fatigue in a woven SiC/SiC ceramic matrix composite with an environmental barrier coating at elevated temperature. International Journal of Fatigue, 170, Article 107543.

[6] Kim, M., et al. (2026). Durability assessment of tile-type reusable thermal protection materials. Materials, 19(2), Article 345.

[7] Le, V. T., et al. (2025). Improved metallic thermal protection systems for re-entry vehicles: Thermomechanical and impact considerations. Journal of Spacecraft and Rockets, 62(4), 1–15.

[8] Uyanna, O., & Najafi, H. (2020). Thermal protection systems for space vehicles: A review on technology development, current challenges and future prospects. Acta Astronautica, 176, 341–356.

[9] Piacquadio, S. (2023). Comprehensive comparison of different integrated thermal protection systems. Aerospace, 10(5), Article 456.

[10] Deriugin, V., et al. (2023). Thermal-structural combined loads design criteria study. NASA.

[11] Peters, A. B., et al. (2024). Materials design for hypersonic Flow. Nature Communications, 15, Article 46753

[12] Gulczyński, M. T. (2023). Combustion chamber fatigue life analysis for reusable liquid rocket engines (Report No. DLR-IB-2023). DLR.

[13] Yang, Z., et al. (2025). Resource and material efficiency in the circular space economy. Chemistry Circularity, Article 00001-5.

[14] Fridh, J. (2023). Health monitoring for highly reusable launch vehicles using machine learning (Report No. 2023-01). Rymdstyrelsen.

[15] Luan, X. (2015). Test methods for investigation of reusable launch vehicle materials under severe environment. MATEC Web of Conferences, 22 [Updated applications 2022–2025].

[16] Saha, S., et al. (2023). Gas permeability mitigation of cryogenically cycled stitched composites using thin plies. Composite Structures, 304, Article 116378.

[17] Trifa, P., et al. (2023). Structural efficiency evaluation of innovative reusable launch vehicles. Journal of Physics: Conference Series, 2526, Article 012116.

[18] Shimizu, L., et al. (2023). Reliability-based damage tolerance framework for achieving highly reusable launch systems. NASA.

[19] Russo, A., et al. (2023). The role of intralaminar damages on the delamination evolution in laminated composite structures. Heliyon, 9(8), Article 02267.

[20] Callister, W. D., & Rethwisch, D. G. (2018). Materials science and engineering: An introduction (10th ed.). Wiley.

[21] ASM International. (1990). ASM handbook, Volume 2: Properties and selection: Nonferrous alloys and special-purpose materials. ASM International.